Eigen modes for the problem of anomalous light transmission through subwavelength holes

B. Sturman and E. Podivilov
Institute of Automation and Electrometry, 630090 Novosibirsk, Russia

M. Gorkunov
Institute of Crystallography, Russian Academy of Sciences, Leninskii pr. 59, 117333 Moscow, Russia

We show that the wide-spread concept of optical eigen modes in lossless waveguide structures, which assumes the separation on propagating and evanescent modes, fails in the case of metal-dielectric structures, including photonic crystals. In addition to these modes, there is a sequence of new eigen-states with complex values of the propagation constant and non-vanishing circulating energy flow. The whole eigen-problem ceases to be hermitian because of changing sign of the optical dielectric constant. The new anomalous modes are shown to be of prime importance for the description of the anomalous light transmission through subwavelength holes.

PACS numbers: 42.25.Bs, 42.25.Fx, 42.70.Qs, 73.20.Mf

The concept of eigenmodes lies at the center of any physical problem for optical light-transmitting systems including waveguides and photonic crystals. This concept seems to be clear and the general properties of the eigen-values and eigen-functions seem to be fully presented in numerous textbooks, see, e.g., [1, 2, 3, 4].

For photonic crystals (PC), determination of the band structures – the eigen-frequencies and eigen-functions versus the wavevector – is the most common. The eigen-frequencies are proven to be real for any lossless PC, i.e., for any periodic distribution of real dielectric optical permittivity $\varepsilon(\mathbf{r})$. A close analogy with the electronic band states is well established [4].

Another formulation of the eigen-mode problem is typical of waveguiding systems which are uniform along the propagation coordinate z: To find the admitted values of the propagation constant β entering the propagation factor $\exp(i\beta z)$ and the corresponding transverse (in x and y) distributions of the optical light fields.

It is known for the lossless dielectric systems ($\varepsilon > 0$) that the admitted values of β^2 are real – positive and negative [1, 2, 3]. The corresponding eigenmodes are propagating and evanescent, respectively, and a close analogy with quantum mechanics holds true. The same is valid for the ideal-metal waveguiding systems, $\varepsilon \to \infty$.

A permanently growing interest to metal-based systems is usually attributed to the excitation of surface plasmons [1, 5] which allow the light constrain on a subwavelength scale. The necessary conditions, $\varepsilon' = \mathrm{Re}\,\varepsilon < -1$, $\varepsilon'' = \mathrm{Im}\,\varepsilon \ll 1$, are fulfilled for many metals. The limit of lossless metal ($\varepsilon' < 0$, $\varepsilon'' = 0$) is as actual as that of lossless dielectric. Recent discovery of the extraordinarily light transmission through subwavelength holes in metal slabs [5, 6] has strongly enhanced the current interest. However, the main ingredients and parametric dependences of this fundamental phenomenon remain poorly understood; its description relies on numerical simulations and simplified models [7, 8, 9, 10].

The present notion of eigenmodes for lossless ($\varepsilon'' = 0$) metal-dielectric waveguide structures (1D and 2D PCs, arrays of holes and single holes in metals, etc.) is surprisingly scarce. It is widely believed that the values of β^2 remain real, i.e. the separation into the propagating and evanescent modes and the analogy with quantum mechanics, still hold true. Using particular models for $\varepsilon(x, y)$ and Fourier expansions, many authors calculate numerically only the real values $\beta^2(\kappa_x, \kappa_y)$, see, e.g., [8, 11] and references therein. To the best of our knowledge, there are only few publications where the authors mention, on the basis of particular calculations, that some of values of β^2 cease to be real [12, 13].

The aim of this letter is (*i*) to show that the generally accepted concept of eigenmodes is insufficient for the case of lossless metal-dielectric waveguide structures, (*ii*) to analyze the general properties of new eigenmodes which are neither propagating nor evanescent, and (*iii*) to demonstrate that these new modes are crucial for the description of the anomalous light transmission through subwavelength holes. We will also pay attention to the propagating modes in the subwavelength case.

To catch the essence of the eigen-mode problem, we consider the case of a 1D PC with ε being a real periodic function of the coordinate x. Restricting ourself to the TH polarization, we have from Maxwell equations for the only nonzero component of the magnetic field $H = H_y$:

$$\hat{L}H = \beta^2 H \ , \quad \hat{L} = \varepsilon \frac{d}{dx}\frac{1}{\varepsilon}\frac{d}{dx} + \varepsilon k_0^2 \ , \qquad (1)$$

where $k_0 = 2\pi/\lambda$. This sets an eigen-mode problem for the operator $\hat{L}$ with β^2 being the eigen-value. The nonzero components of the light electric field are expressed by H: $E_x = \beta H/\varepsilon k_0$, $E_z = (i/\varepsilon k_0)\, dH/dx$.

The conclusion about reality of β^2 and analogy with quantum mechanics is generally based on Hermitian character of the differential operator $\hat{L}$, i.e., on the property $\langle H_2|\hat{L}H_1\rangle = \langle H_1|\hat{L}H_2\rangle^*$, where $\langle ..|..\rangle$ stands for the scalar product. The only possibility to get this property is to define the scalar product of two complex functions H_1 and H_2 as

$$\langle H_2|H_1\rangle = \int \varepsilon^{-1}(x)\ H_2^*(x)\, H_1(x)\, dx \ . \qquad (2)$$

In the dielectric case, $\varepsilon(x) > 0$, this definition meets all axioms of the scalar product [14]. For sign-changing func-

tions $\varepsilon(x)$, it contradicts, however, to one of the axioms – the norm $\langle H|H\rangle$ ceases to be positively defined. Therefore, the conclusions about Hermitian character of $\hat{L}$ and about reality of β^2 cannot be made.

Apart from the above negative observation, some positive assertions can be made:

– If an eigen-function possesses a positive norm, the corresponding value of β^2 is real. Two eigen-functions H_1 and H_2 corresponding to different real eigenvalues β_1^2 and β_2^2 are orthogonal, $\langle H_2|H_1\rangle = 0$. If at least one of $\beta_{1,2}$ is complex, it has to be replaced by $\langle H_2^*|H_1\rangle = 0$.

– In the case of TE polarization (nonzero E_y, H_x, and H_z components) the above peculiarities are absent – the admitted values β^2 are real and an analogy with quantum mechanics holds true.

– In the 2D case, Hermitian character of the eigen-mode problem and reality of β^2 can be proven in exceptional cases of waves with $E_z = 0$ (TE modes). In the general case (TM and hybrid modes) complex values of β^2, i.e., anomalous modes, are present, see also below.

Now we turn to particular examples. Consider first a 1D PC consisting of an alternating sequence of layers with permittivities $\varepsilon_{1,2}$ and thicknesses $x_{1,2}$; the period is $x_0 = x_1 + x_2$. Solution of Eq. (1) for an eigenmode has the form $H(x) = e^{i\kappa x}\, h(x)$, where κ is the Bloch wavevector ranging from $-\pi/x_0$ to π/x_0 and $h(x)$ is an x_0-periodic function. Using continuity of $H(x)$ and $E_z(x) \propto \varepsilon^{-1}\, dH/dx$ at the interfaces and periodicity of $h(x)$ and dh/dx, we obtain the following dispersion equation for β^2 (it generalizes Eq. (13) of [12]):

$$\frac{1}{2}\left(\frac{p_1\varepsilon_2}{p_2\varepsilon_1} + \frac{p_2\varepsilon_1}{p_1\varepsilon_2}\right)\sin(p_1x_1)\,\sin(p_2x_2) = \cos(p_1x_1)\,\cos(p_2x_2) - \cos(\kappa x_0)\;, \tag{3}$$

where $p_{1,2} = (\varepsilon_{1,2}k_0^2 - \beta^2)^{1/2}$. The trigonometric functions possess generally complex arguments. If $\varepsilon_{1,2}$ are real, Eq. (3) is real as well. The roots $\beta = \pm\sqrt{\beta^2}$ describe the wave propagation in the $\pm z$ directions.

The circles in Fig. 1a show the values of the propagation constant on the complex β', β'' plane in the lossless case for $\kappa = 0$ (at the center of the Brillouin zone), $x_1 = x_0/5 = \lambda/4$, $\varepsilon_1 = 1$, and $\varepsilon_2 = -9.6$. The last parameter corresponds to silver at $\lambda \approx 0.5$ μm [15]. We have a single real root, $\beta/k_0 \approx 1.2$, and two sequences of roots with $\beta'' \neq 0$. One sequence, with pure imaginary values of β, refers to the known evanescent modes. Another sequence, with $\beta' \neq 0$ and $\beta'' \gtrsim \sqrt{|\varepsilon_2|}$ (complex values of β^2) corresponds to *anomalous modes* forbidden in the dielectric case. They combine features of propagating and evanescent modes. The symmetric pairs of anomalous roots correspond to mutually conjugate values of β^2.

At $\kappa = 0$, the modes are either even, $h(x) = h(-x)$, or odd, $h(x) = -h(-x)$; the "even" and "odd" roots are shown by filled and open circles in Fig. 1a. The single real root corresponds to the even propagating mode. About 30% of the modes are anomalous.

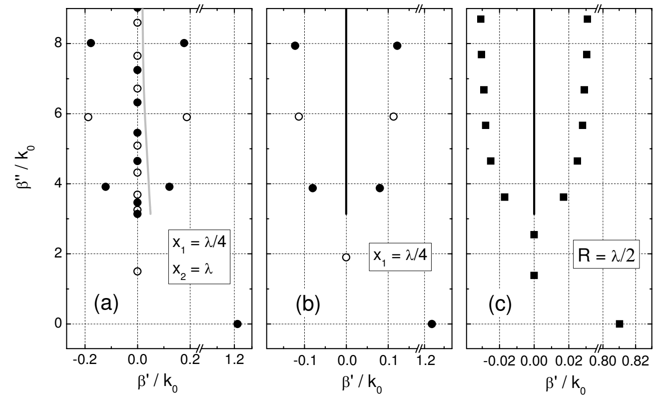

FIG. 1: Values of β for $\varepsilon_2 = -9.6$ and three structures: (a) 1D PC with $x_2 = 4x_1$ (the gray line shows positions of evanescent roots for $\varepsilon_2'' = 0.3$); (b) a single slit with $x_1 = \lambda/4$; (c) a single cylindric hole with $R = \lambda/2$. The vertical solid lines in (b) and (c) show the continuous spectrum.

With weak losses taken into account, the roots experience small displacements. The strongest of them (shifts to the right) occur for the evanescent roots. The gray line in Fig. 1a shows positions of these roots for $\varepsilon_2'' = 0.3$, which models silver at ≈ 0.5 μm. The other displacements do not exceed the circle size.

Whereas the Pointing vector $\mathbf{P} = (P_x, P_z)$ is zero for the evanescent modes, it is nonzero for the anomalous modes. Each anomalous mode is responsible thus for circulation of the light energy. Applying the orthogonality relation $\langle H_2^*|H_1\rangle = 0$ to a conjugate pair of anomalous modes, we come to the following relation for an anomalous eigen-function $h_a(x)$:

$$\int \varepsilon^{-1}(x)\;|h_a(x)|^2\;dx = 0\;, \tag{4}$$

where the integration occurs over a period of x_0. Since $P_z \propto \beta'\varepsilon^{-1}(x)\,|h(x)|^2\exp(-2\beta'' z)$, it shows that the x-averaged energy flux is zero for the anomalous modes – the inflow in air is compensated by the outflow in metal. Eq. (4) can be interpreted also as a zero norm for the eigen-vector $h_a(x)$. The eigen-vectors $h(x)$ for the propagating and evanescent modes possess positive norms. Fig. 2 shows the energy circulation within a half-period $x_0/2$ for the first anomalous mode with $\beta' > 0$. For the mode with $\beta' < 0$ the arrows have to be inverted.

What happens with the above modes when changing $x_{1,2}$? With decreasing slit width x_1, the propagating mode survives (β' grows as x_1^{-1}), the evanescent mode with $\beta'' < \sqrt{|\varepsilon_2|}$ disappears, the other evanescent modes experience minor changes, and the vertical distance between the anomalous modes increases as $2\pi/x_1$.

Increasing wall parameter x_2 does not affect strongly the propagating and anomalous modes in Fig. 1a. However, the density of evanescent modes in the region $\beta'' > \sqrt{|\varepsilon_2|}$ increases $\propto x_2$. The limit $x_2 \to \infty$ corresponds

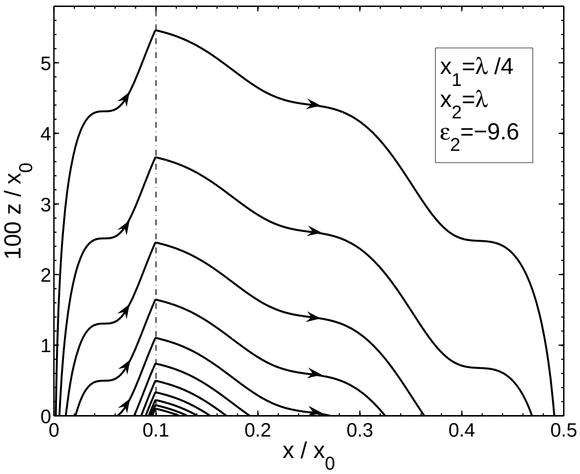

FIG. 2: Streamlines of the Pointing vector for the first anomalous symmetric mode with $\beta' > 0$.

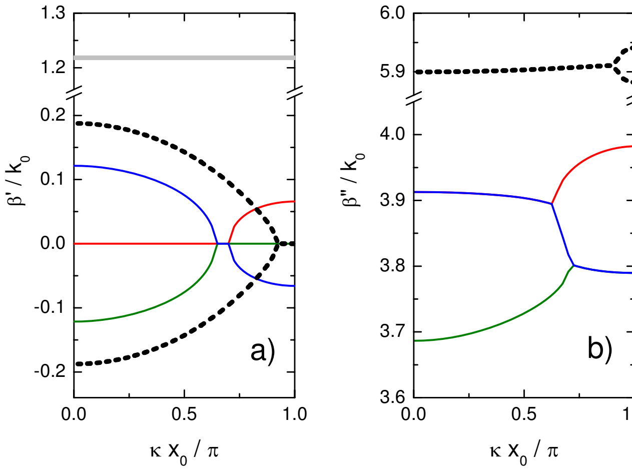

FIG. 3: Dependences $\beta''(\kappa)$ and $\beta'(\kappa)$ for the periodic structure with $x_0 = 5x_1 = 5\lambda/4$, and $\varepsilon_2 = -9.6$. Solid lines are plotted for the first pair of anomalous modes and the nearest evanescent mode, the dotted lines correspond to the second anomalous pair, and the gray line is for the propagating mode.

to the single-slit case. It is represented by Fig. 1b. We have single localized (in $|x|$) propagating and evanescent modes, a sequence of localized anomalous modes, and a continuous spectrum of non-localized evanescent modes with $\beta' = 0$ and $\beta'' > \sqrt{|\varepsilon_2|}$. This also follows from a direct description of the single-slit case. The anomalous modes represent thus properties of a single-hole.

For $k_0x_1 \ll 1$, $x_2 \to \infty$ (very narrow single slit) we have for the single propagating mode and $\varepsilon_2'' \ll |\varepsilon_2'|$:

$$\beta \simeq \frac{1}{x_1}\left[\ln\left(\frac{|\varepsilon_2'|+1}{|\varepsilon_2'|-1}\right) + \frac{2i\,\varepsilon_2''}{|\varepsilon_2'|^2-1}\right]. \qquad (5)$$

The effective refractive index β'/k_0 tends to infinity for $x_1 \to 0$. In the ideal-metal limit ($|\varepsilon_2| \to \infty$) we have $\beta = 0$. For $x_{1,2} \to \infty$ the propagating mode transforms to the usual surface plasmon.

The eigen-functions for the above periodic and single-slit cases (localized and delocalized) can be constructed readily from the exponential functions $\exp(ip_{1,2}x)$ with proper values of $p_{1,2}(\beta^2)$.

The Bloch dependences $\beta'(\kappa)$ and $\beta''(\kappa)$ for the propagating and evanescent modes, which are present in the PC literature, are insufficient in the metal-dielectric case where the anomalous modes are present. Moreover, the anomalous modes cause strong interaction of different branches and peculiarities of Bloch diagrams. Fig. 3 shows examples of the κ-dependences for our 1D PC structure. The value of $|\beta'|$ for the first pair of anomalous modes (see Fig. 1a) decreases with growing κ and turns to zero for $0.66 \lesssim \kappa x_0/\pi \lesssim 0.71$, i.e., the anomalous modes become evanescent within this interval. For $\kappa x_0/\pi \gtrsim 0.71$ a pair of anomalous modes appears again. This behavior is correlated with bifurcations of $\beta''(\kappa)$ for the anomalous modes and the nearest evanescent mode. Behavior of the second pair of anomalous modes is different. The confluence of $\beta'(\kappa)$ for these modes at $\kappa x_0/\pi \simeq 0.9$ is accompanied by the split of $\beta''(\kappa)$. The dependence $\beta(\kappa)$ for the propagating mode and most of evanescent modes is fairly weak.

The situation described is also inherent in 2D structures. Consider for simplicity TM ($H_z = 0$) modes for a cylindric hole of radius R in a lossless metal. The corresponding dispersion equation reads [16]

$$p_2\, J_1\, H_0^{(1)} - \varepsilon_2 p_1\, J_0\, H_1^{(1)} = 0\,, \qquad (6)$$

where $J_{0,1} = J_{0,1}(p_1R)$ and $H_{0,1}^{(1)} = H_{0,1}^{(1)}(p_2R)$ are the Bessel and Hankel functions. Fig. 1c shows the spectrum of β for $\varepsilon_2 = -9.6$ and $R = \lambda/2$. One propagating mode, two evanescent modes, a sequence of localized anomalous modes, and a continuous spectrum are present.

The TM propagating mode exists here only for $R > R_{min}(\varepsilon_2)$ with R_{min} decreasing from $\simeq 0.334\lambda$ to $\simeq 0.257\lambda$ when ε_2 changes from -10 to -1. For the HE$_{11}$ propagating mode, which provides the minimum cut-off, R_{min} decreases from $\simeq 0.22\lambda$ to $\simeq 0.087\lambda$ in this range of ε_2. For the ideal metal $R_{min}/\lambda \simeq 0.3$. As follows from Eq. (6), in the range $-1 < \varepsilon_2 < 0$ a propagating mode exists even for $R \to 0$.

To show the importance and applications of our approach, we consider the following fundamental problem: An x-polarized plane wave of a unit amplitude is incident normally onto the above 1D metal-dielectric PC occupying the semi-space $z > 0$. It is necessary to determine the transmission properties at the interface $z = 0$.

We use the following explicit mode expansion for H:

$$H = \begin{cases} \sum\limits_{\nu=0}^{\infty} a_\nu h^\nu(x)\, e^{i\beta_\nu z}\,; & z > 0 \\ e^{ik_0 z} + \sum\limits_{n=-\infty}^{\infty} b_n\, e^{inKx + q_n z}\,; & z < 0\,, \end{cases} \qquad (7)$$

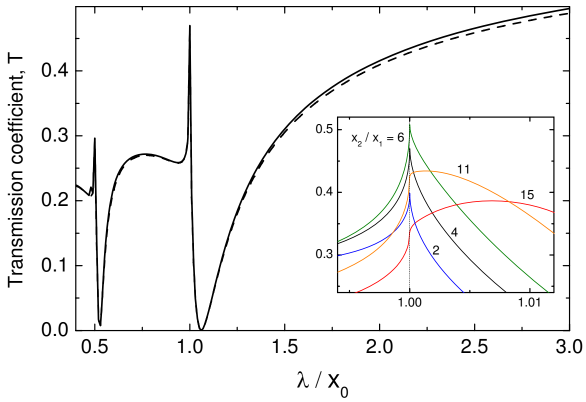

FIG. 4: Dependence $T(\lambda/x_0)$ for $\varepsilon_2' = -9.6$, $x_2/x_1 = 4$, and $N = 48$; the solid and dashed lines are plotted for $\varepsilon_2'' = 0$ and 0.3. The inset shows $T(\lambda/x_0)$ for $\varepsilon_2'' = 0$ and five values of x_2/x_1 in the vicinity of the main peak.

where ν numerates the even eigen-modes at $\kappa = 0$, $K = 2\pi/x_0$, $q_n = (n^2K^2 - k_0^2)^{1/2}$ for $n^2K^2 > k_0^2$, $q_n = -i\,(k_0^2 - n^2K^2)^{1/2}$ for $k_0^2 > n^2K^2$, and b_n and a_ν are the amplitudes to be found. Real and imaginary values of q_n correspond to evanescent and propagating waves in air. With increasing period, new diffraction orders appear at $x_0 = n\lambda$ in reflected light; only a single propagating wave (with $n = 0$) is allowed for $x_0 < \lambda$.

Employing the boundary conditions at the interface $z = 0$ and the Fourier transformation, we come to the set of linear algebraic equations for determination of a_ν:

$$\sum_{\nu=0}^{\infty} a_\nu \left[h_n^\nu - i\,\beta_\nu q_n^{-1}\,(h^\nu/\varepsilon)_n \right] = 2\delta_{n0}\,, \tag{8}$$

where h_n^ν and $(h^\nu/\varepsilon)_n$ are the Fourier components of the periodic functions $h^\nu(x)$ and $h^\nu(x)/\varepsilon(x)$. These components were expressed explicitly through β_ν.

A numerical routine with truncation of this set at $\nu_{max} = n_{max} = N \gg 1$ was used to calculate a_ν and determine the reflection and transmission properties. The results of calculations converge perfectly well with increasing N when all eigen-modes are taken into account. However, the calculation results *diverge when the anomalous modes are ignored*. This means (i) that the set of the eigen-functions is incomplete without the anomalous modes and (ii) that these modes are directly involved in the energy transfer from the incident plane wave to the propagating mode(s) inside the slits.

Consider the key results for the transmission coefficient T defined as the energy-flax fraction transmitted into the propagating mode at $z = 0$. This definition is useful even for $\varepsilon'' \neq 0$ when the propagating mode decays inside the metal as $\exp(-2\beta'' z)$. Fig. 4 shows the dependence $T(\lambda)$ for the lossless and lossy cases. The losses influence T very weakly; their main effect occurs during propagation. The function $T(\lambda)$ possesses narrow peaks at $\lambda = x_0/n$; the main peak corresponds to $n = 1$. The geometric nature of the resonances is evident and it is not overshadowed by the Fabry-Perot interference typical of the slab case [7]. The maximum value of the transmission coefficient, $T_{max} \simeq 0.47$ (which corresponds to $x_1 = \lambda/5$) is pretty high. It is decreasing slowly with increasing $|\varepsilon_2|$. For $\lambda > x_0$, the difference $1 - T$ is the reflection coefficient.

Our procedure allows to resolve the fine structure of the main peak and investigate the dependence T_{max} on the ratio x_2/x_1, see the inset in Fig. 4. The structure is different for $x_2/x_1 < |\varepsilon_2|$ and $x_2/x_1 > |\varepsilon_2|$. In the first case, the peak spike is sharp and centered exactly at $\lambda = x_0$. In the second case, the right wing of the peak is broadened and the very maximum is slightly shifted to the right. Surprisingly, $T_{max}(x_1/x_2)$ *is not* a monotonously increasing function; the optimum value of x_1/x_2 is $\simeq 1/6$ where $T_{max} \simeq 0.51$. Note that the effective permittivity of our medium in the limit $\lambda \gg x_0$ is $\langle \varepsilon^{-1} \rangle^{-1} = |\varepsilon_2| x_0/(x_1|\varepsilon_2| - x_2)$, see, e.g., [17]; it turns to infinity and changes sign at $x_2/x_1 = |\varepsilon_2|$. Validity of this limiting case was controlled numerically.

In conclusion, the eigen-mode problem for metal-dielectric structures – photonic crystals, single holes in a metal – is essentially different from that typical of dielectric structures and quantum mechanics. It is not hermitian and the eigen-values for the localized states are generally complex in the lossless case. The anomalous transmission through subwavelength holes is substantially determined by the transmission coefficient for a single interface. This characteristic possesses a number of fundamental features. The opposite faces of the metal-dielectric structure are coupled via a weakly decaying propagating mode.

[1] A. Yariv and P. Yeh, *Optical waves in crystals*, Wiley Interscience, Ch. 11, (2003).

[2] C. Vassalo, *Optical waveguide concepts*, Elsevier, Oxford (1991).

[3] R. E. Collin, *Field theory of guided waves*, Wiley Interscience (1991).

[4] J. D. Joannopoulos, R. D. Meade, and J. N. Winn, *Photonic crystals*, Princeton University Press (1995).

[5] W. L. Barnes, A. Dereux, and T. W. Ebbesen, Nature, **424**, 824 (2003).

[6] T. W. Ebbesen et al., Nature **391**, 667 (1998).

[7] J. A. Porto, F. J. Garcia-Vidal, and J. B. Pendry, Phys. Rev. Lett. **83**, 2845 (1999); F. J. Garcia-Vidal and L. Martin-Moreno, Phys. Rev. B **66**, 155412 (2002).

[8] M. M. J. Treacy, Phys. Rev. B **66**, 195105 (2002).

[9] P. Lalanne, J. P. Hugonin, and J. C. Rodier, Phys. Rev. Lett. **95**, 263902 (2005).

[10] Y. Xie, et al., Opt. Express, **14**, 6400 (2006).

[11] S. G. Tikhodeev et al., Phys. Rev. B **66**, 045102 (2002).
[12] P. Sheng, R. S. Stepleman, and P. N. Sanda, Phys. Rev. B **25**, 2907 (1982).
[13] D. M. Whittaker and I. S. Culshaw, Phys. Rev. B **60**, 2610 (1999).
[14] J. Mathews and R. L. Walker, *Mathematical methods of physics*, W. A. Benjamin, INC. (1964), Ch, 6.
[15] P. B. Jonson and R.W. Christy, Phys. Rev. B **6**, 4370 (1972).
[16] C. A. Pfeiffer, E. N. Economou, and K. L. Ngai, Phys. Rev. B **10**, 3038 (1974).
[17] A. Yariv and P. Yeh, J. Opt. Soc. Am. **67**, 423 (1977).